MOLECULAR AND CELLULAR BIOLOGY, Apr. 2006, p. 2519–2530 Vol. 26, No. 7
0270-7306/06/$08.00+0 doi:10.1128/MCB.26.7.2519–2530.2006

pVHL Function Is Essential for Endothelial Extracellular Matrix Deposition

Nan Tang,[1,2] Fiona Mack,[3] Volker H. Haase,[4] M. Celeste Simon,[3] and Randall S. Johnson[1]*

Molecular Biology Section, Division of Biological Sciences,[1] and Molecular Pathology Graduate Program,[2] University of California—San Diego, La Jolla, California 92093, and Abramson Family Cancer Research Institute[3] and Renal-Electrolyte and Hypertension Division,[4] University of Pennsylvania School of Medicine, Philadelphia, Pennsylvania 19104

Received 3 October 2005/Returned for modification 16 November 2005/Accepted 3 January 2006

The tumor suppressor von Hippel-Lindau protein (pVHL) is critical for cellular molecular oxygen sensing, acting to target degradation of the hypoxia-inducible factor alpha transcription factor subunits under normoxic conditions. We have found that independent of its function in regulating hypoxic response, the VHL gene plays a critical role in embryonic endothelium development through regulation of vascular extracellular matrix assembly. We created mice lacking the VHL gene in endothelial cells; these conditional null mice died at the same stage as homozygous VHL-null mice, with similar vascular developmental defects. These included defective vasculogenesis in the placental labyrinth, a collapsed endocardium, and impaired vessel network patterning. The defects in embryonic vascularization were correlated with a diminished vascular fibronectin deposition in vivo and defective endothelial extracellular fibronectin assembly in vitro. We found that the impaired migration and adhesion of VHL-null endothelial cells can be partially rescued by the addition of back exogenous fibronectin, which indicates that pVHL regulation of fibronectin deposition plays an important functional role in vascular patterning and maintenance of vascular integrity.

The von Hippel-Lindau (VHL) hereditary cancer syndrome is caused by germ line mutation of the VHL tumor suppressor gene (26). Clear-cell carcinomas of the kidney (renal cell cancers), angiomas of the retina, and hemangioblastomas of the central nervous system are very common in these patients. Other tumors, such as pheochromocytomas, endolymphatic sac tumors, islet cell tumors of the pancreas, and vascular tumors in non-central-nervous-system sites are also found in these patients (26). Individuals with VHL disease typically have inherited a defective VHL allele. The remaining wild-type (wt) VHL allele is either inactivated or lost in tumors, obeying the Knudsen two-hit hypothesis model for tumor suppressor function.

The von Hippel-Lindau tumor suppressor protein (pVHL) plays an important role in the oxygen-sensing pathway. At a molecular level, pVHL forms complexes with elongin C, elongin B, and cullin-2, which structurally resemble SCF-like ubiquitin ligases in yeast (10, 29, 45). In the presence of oxygen, two proline residues of hypoxia-inducible factor alpha (HIF-α) subunits are hydroxylated by prolyl hydroxylases (6, 13, 27). This facilitates pVHL complex binding and targets HIF-α subunits for degradation by the proteasome (33). Under hypoxic conditions, the prolyl hydroxylation of HIF-α subunits is inhibited, which allows HIF-α subunits to escape ubiquitin-mediated proteolysis. Thus, HIF-α subunits accumulate, translocate to the nucleus, and then form heterodimeric transcription factors with the aryl hydrocarbon receptor nuclear translocator (also called HIF-1β).

Many hypoxia-inducible genes, including vascular endothelial growth factor (VEGF), glucose transporter 1 (GLUT-1), and erythropoietin, are regulated by HIF-α at a transcriptional level (19, 24, 32, 43). Several groups have shown that cells lacking pVHL are unable to degrade HIF-α subunits in the presence of oxygen, which in turn leads to excessive transcription of HIF-α target genes (24). In VHL patients with hemangioblastomas and renal cell cancers, tumors are typically highly vascularized and are known to overproduce the HIF-α target and the angiogenic factor VEGF (32). Furthermore, these tumors occasionally overproduce the hormone erythropoietin. These results all strongly suggest the close relationship between VHL-induced tumors and the dysregulation of HIF. But a recent study suggested that although loss of VHL alone is sufficient to dysregulate HIF, other genetic changes are necessary to facilitate VHL-mediated tumorigenesis in fibrosarcoma tumor models (31). Whether this is true in other cell types requires further investigation.

In addition to its role in HIF-α regulation, pVHL binds to other cellular proteins, and modulates these proteins in ways that are independent of polyubiquitination. pVHL has also been found to be important for extracellular matrix assembly (5, 14, 35, 37). Fibronectin (FN) staining is greatly reduced in VHL-null mouse embryos (37). Renal carcinoma cells lacking pVHL secrete fibronectin but fail to produce a recognizable extracellular fibronectin matrix (37). It has been found that pVHL can bind to fibronectin and that pVHL-deficient cells cannot assemble organized macroscopic fibronectin arrays, although they can still secrete fibronectin. pVHL can also form protein complexes with specific isoforms of protein kinase C and prevent the translocation of protein kinase Cδ and -ζ to cell membrane (38). Finally, it has been found that pVHL can bind to and suppress the Sp1 transcription factor, although there is no evidence that pVHL targets Sp1 for degradation (7, 34).

* Corresponding author. Mailing address: Molecular Biology Section, MC-0377, Division of Biological Sciences, University of California—San Diego, La Jolla, CA 92093-0377. Phone: (858) 822-0509. Fax: (858) 822-5833. E-mail: rjohnson@biomail.ucsd.edu.

In the fly, inactivation of VHL by RNA interference causes breakdown of the main embryonic vasculature, with excessive looping of smaller branches (3). VHL-deficient ($VHL^{-/-}$) mice fail to develop embryonic vasculature in the placenta, and this results in an embryonic lethality around embryonic days 10.5 to 12.5 (E10.5 to E12.5) (18). These findings suggest an important role for VHL in vascular development.

Although much is known about the effects of loss of VHL in the tumor cell, comparatively little is understood about its role in the blood vessel itself. In recent work, we have shown that loss of HIF-1α in the endothelial cell (EC) results in deficiencies in tumor formation and wound healing (48). We show here that loss of VHL, a key negative regulator of HIF-1, acts outside of the HIF-1 pathway, with striking effects on endothelial cell extracellular matrix deposition.

MATERIALS AND METHODS

Animals and embryo dissection. Animals were housed in an Association for Assessment and Accreditation of Laboratory Animal Care-approved facility in filter-topped cages and provided with food and water. All animal experiments were conducted using the highest standards for humane care in accordance with the National Research Council's *Guide for the Care and Use of Laboratory Animals*. Endothelial cell-specific inactivation of VHL and HIF-1α was achieved by cross-breeding Tie2-Cre transgenic mice (30) with mice harboring two alleles of exon 1 of VHL flanked by *loxP* sites ($VHL^{+f/+f}$) (20) or mice harboring VHL and HIF-1α, which both are flanked by *loxP* sites ($VHL^{+f/+f}$ $HIF\text{-}1\alpha^{+f/+f}$) (42). To generate VHL EC-null embryos, homozygous $VHL^{+f/+f}$ females were mated with heterozygous $VHL^{+f/wt}$ Tie2-Cre^{+} males. To generate HIF-1α and VHL EC-null mice, homozygous $VHL^{+f/+f}$ $HIF\text{-}1\alpha^{+f/+f}$ females were mated with $VHL^{+f/wt}$ $HIF\text{-}1\alpha^{+f/+f}$ Tie2-Cre^{+} males. DNA isolated from the tails of embryos was used for genotyping animals. The embryos were dissected from the yolk sacs at E9.5, E10.5, E11.5, E12.5, and E13.5. All the embryos for later histological examination were live with their hearts beating while they were dissected from the yolk sacs. The placentas were dissected and fixed overnight at 4°C with 4% paraformaldehyde prior to paraffin wax embedding, sectioning, and staining with hematoxylin and eosin (H&E). Mox2-Cre transgenic mice were purchased at the Jackson Laboratory (47).

Whole-mount CD31 staining. CD31 staining was carried out as previously described by Ryan et al. (42). Embryos were dissected from the yolk sac at E9.5, E10.5, E11.5, and E12.5 and fixed overnight in 4% paraformaldehyde at 4°C. After being blocked in PBSBT (3% bovine serum albumin [BSA], 0.1% Triton X-100, and phosphate-buffered saline [PBS]) for 1 h, the embryos were incubated overnight with biotinylated rabbit anti-CD31 antibody MEC13.3 (Pharmingen) diluted 1:50 in PBSBT at 4°C. On the next day, after several washes, biotin was detected with a Vectastain kit with ABC-HRP (avidin-biotinylated horseradish peroxidase) reagents (Vector Laboratories, Inc). The peroxidase staining was visualized by using a DAB kit (Vector Laboratories, Inc). The pictures were taken by a dissection microscope.

Immunohistochemistry. Mouse E11.5 and E12.5 embryos were dissected from yolk sacs. Overnight incubation of antifibronectin (1:400; Sigma) was performed on serial paraffin sagittal sections of embryos (Vector Laboratories). Staining was visualized with an ABC alkaline phosphatase kit with Vector Blue as a substrate. For yolk sac paraffin sections, overnight incubation of antifibronectin (1:400; Sigma) was performed on sections, followed by a 1-h incubation of fluorescein isothiocyanate (FITC)-conjugated anti-rabbit secondary antibody (Santa Cruz).

In vitro endothelial cell culture, adhesion assay, migration, and permeability assay. Mouse lung endothelial cells were isolated from $VHL^{+f/+f}$ and $VHL^{+f/+f}$ $HIF\text{-}1\alpha^{+f/+f}$ mice and cultured as previously described (48). A culture medium with 20% fibronectin-depleted serum was used. Fibronectin was depleted by gelatin-Sepharose (Amersham), which is widely used to purify FN and to yield a FN-depleted serum with a good growth supplement for numerous cells (40). All the experiments were performed on the second passage of primary lung ECs.

For the adhesion assay, 48-well plates were coated with either 5-μg/well fibronectin (BD Biosciences) or PBS at 37°C for 1 h. A total of 5×10^4 ECs harvested by brief (1-min) treatment with trypsin, followed by neutralization with fibronectin-free serum, were washed with PBS and resuspended in 200 μl of adhesion buffer (serum-free culture medium containing 0.5% BSA). ECs were plated in the wells and allowed to attach for 90 min. Cells were then gently washed three times with adhesion buffer to remove nonadherent cells, and the adherent cells were stained with a 0.1% crystal violet solution at room temperature for 2 min. After being washed three times, the insoluble dye taken up by adherent cells was dissolved in 200 μl of methanol, and the absorbance of the solution was read at 595 nm in an enzyme-linked immunosorbent assay plate reader.

For the paracellular permeability assay, wild-type, $VHL^{-/-}$, and $VHL^{-/-}$ $HIF\text{-}1\alpha^{-/-}$ ECs were cultured to form a monolayer on fibronectin-coated polycarbonate transwells (24 wells; pore size, 0.3 μm; Corning Costar Corp., Cambridge, MA). The permeability through endothelial cell monolayers was investigated by the addition of dextran-fluorescein isothiocyanate (molecular weight, 40S; Sigma) to the upper transwells at a final concentration of 1 mg/ml. After 3 h, 50-μl samples were taken from the bottom chambers to measure fluorescence (absorption wavelength, 492 nm; emission wavelength, 520 nm). All experiments were performed in triplicate.

Migration assay was performed as described previously (48). Wild-type, $VHL^{-/-}$, and $VHL^{-/-}$ $HIF\text{-}1\alpha^{-/-}$ endothelial cells were plated on either fibronectin-coated or collagen-coated transwells. Cells were allowed to migrate to 5% fetal calf serum for 24 h. Data were expressed as one triplicate culture experiment ± the standard error of the mean (SEM).

Preparation of RNA. Endothelial cells were cultured under normoxic (20% O_2) or hypoxic (0.5% O_2) conditions for 8 h. After that, cells were washed twice with cold PBS before direct extraction of total RNA with a QIAGEN RNeasy kit, according to the manufacturer's protocol.

Quantitative real-time PCR analysis. One microgram of total RNA was used to synthesize the first-strand cDNA from random hexamer primers with Superscript First-Strand (Invitrogen, Carlsbad, CA) according to the manufacturer's protocol. After synthesis of cDNA, gene expression of VEGF, phosphoglycerate kinase (PGK), GLUT-1, inducible nitric oxide synthase (iNOS), Tie2, Ang-1, Ang-2, and endothelial NO synthase (eNOS) was quantified by real-time PCR. Results were normalized to the expression level of ribosome RNA, as described previously (48). The forward (F) and reverse (R) primers and probes (P) labeled with fluorescence dye are listed below; VEGF, PGK, and GLUT-1 were previously described (48).

For Tie2, F is 5′-AACCAACAGTGATGTCTGGTCCTAT-3′, R is 5′-GCACGTCATGCCGCAGTA-3′, and Tie2/P is 5′-(6-FAM)-TGCCTCCTAAGCTAACAATCTCCCAGAGCAATA-(TAMRA)-(phosphate)-3′, where FAM is 6-carboxyfluorescein and TAMRA is 6-carboxytetramethylrhodamine. For iNOS, F is 5′-ACCCTAAGAGTCACAAAATGGC-3′, and R is 5′-TTGATCCTCACATACTGTGGACG-3′. For eNOS, F is 5′-CCTTCCGCTACCAGCCAGA-3′, and R is 5′-CAGAGATCTTCACTGCATTGGCTA-3′. For Ang-1, F is 5′-GCAAATGCGCTCATGCTA-3′, (R) 5′-GGAGTAACTGGGCCCTTTGAA-3′, and P is 5′-FAM-CAGCAGCATGACCTAATGGAGACCGTC. For Ang-2, F is 5′-TGACAGCCACGGTCAACAAC-3′, R is 5′-ACGGATAGCAACCGAGCTCTT-3′, and P is 5′-FAM-CAGCAGCATGACCTAATGGAGACCGTC-3′.

Immunofluorescence staining. Wild-type and null EC were plated on Lab-Tek II chamber slides and allowed to grow for 1 week in fibronectin-depleted culture medium. After being washed several times in PBS, the cells were fixed in acetone at −20°C for 20 min. The slides were then blocked by PBSBT for 1 h, followed by overnight incubation of a 1:400 dilution of polyclonal rabbit antifibronectin antibody (Sigma) at 4°C. The following day, after several washes with PBS, the slides were incubated with FITC-conjugated anti-rabbit antibody diluted 1:200 (Vector) in PBSBT for 1 h. Then the slides were washed with PBS several times and stained with 4′-6-diamidino-2-phenylindole hydrochloride (DAPI) (0.5 μg/ml) for 5 min. The staining was examined under a fluorescence microscope.

Statistical analysis. Statistical significance was determined by an unpaired *t* test ($P = 0.05$), using StatView 5.0.

RESULTS

VHL EC-null embryos die in utero at E12.5. To study VHL function in ECs, mice harboring two alleles of exon 1 of VHL flanked by loxp sites ($VHL^{+f/+f}$) were bred with transgenic mice expressing Tie2-Cre (21, 30) to get $VHL^{+f/+f}$ Tie2-Cre (VHL EC-null) mice. A total of 92 mice (from 21 litters) were genotyped; no VHL EC-null mice were found, demonstrating in utero lethality. By breeding homozygous $VHL^{+f/+f}$ female mice with $VHL^{+f/wt}$ Tie2-Cre^{+} male mice, we were able to generate $VHL^{+f/+f}$ Tie2-Cre^{+} (VHL EC-null) embryos. A total of 12 litters collected from this breed scheme were examined between E8.5 and E13.5. VHL EC-null embryos appeared

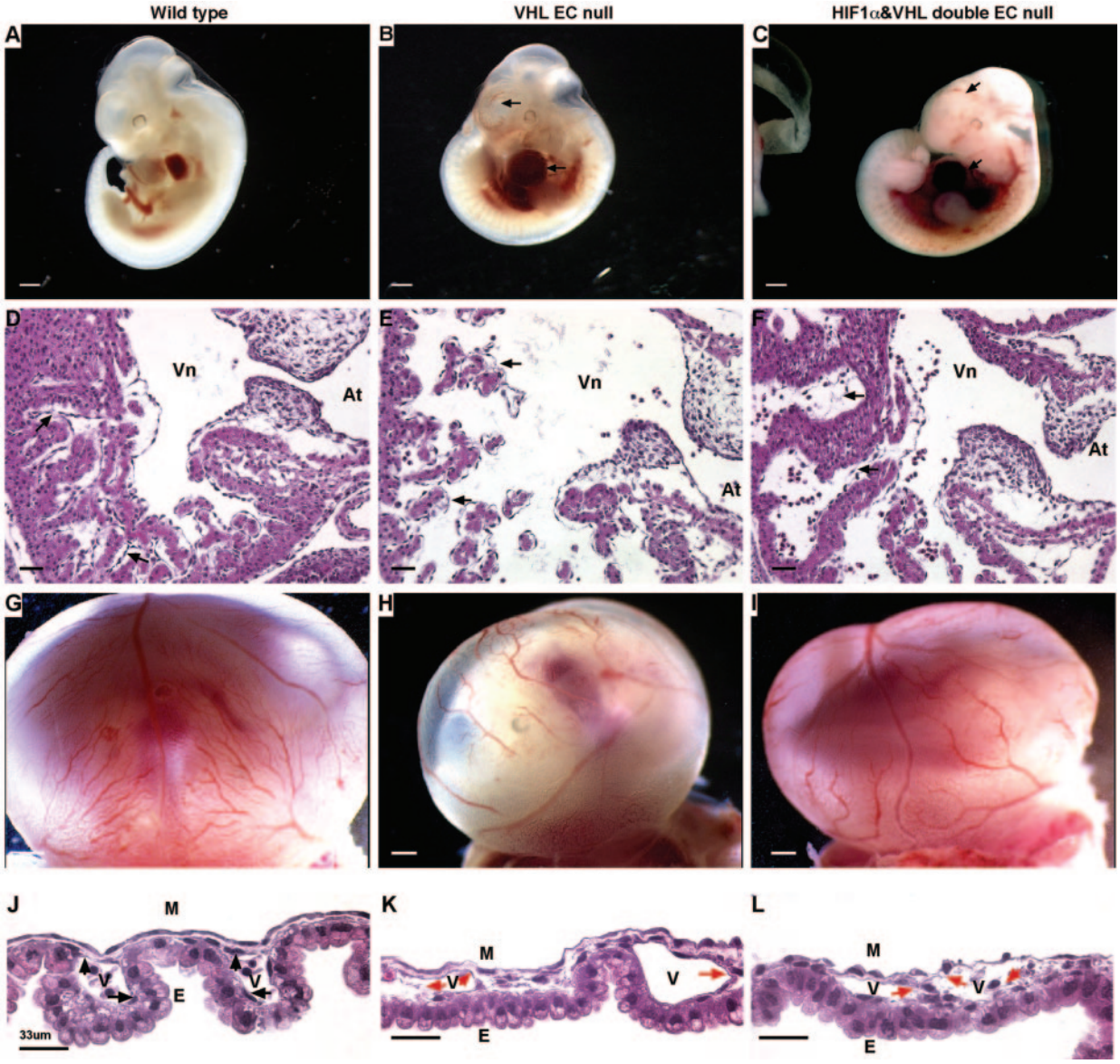

FIG. 1. Phenotypic defects in VHL EC-null and VHL/HIF-1α EC double-null embryos. (A to C) Hemorrhage (black arrows) in the head and heart is a common feature in VHL EC-null (B) and HIF-1α and VHL EC double-null embryos (C) compared with wild-type embryos (A) at E12.5. Bar, 500 μm. (D to F) H&E staining of the heart sagittal sections of wild-type (D), VHL EC-null (E) and VHL HIF-1α EC double-null embryos (F) at E11.5. Black arrows indicate endocardial endothelium; red arrows indicate myocardial trabeculae. Bar, 12.5 μm. (G to I) Gross morphology of whole-mount yolk sacs from the wild-type (G), VHL EC-null (H), and VHL HIF-1α EC double-null (I) mouse embryos at E11.5. (G) Yolk sac vessels from wild-type embryos display differentiated vasculature composed of large- and small-diameter vessels, like branches of trees. These branches form an organized yolk sac vascular network. The vessels of yolk sacs from EC-null embryos are not well organized and connected. Bar, 500 μm. (J to L) H&E staining of yolk sac sections of wild-type (J), VHL EC-null (K), and VHL HIF-1α EC double-null embryos (L). M, mesodermal layer of cells lying on the endothelium; E, endodermal layer of cells underlying the endothelium; V, vitelline blood vessels. Wild-type endothelium (black arrows) maintains tight contact with the surrounding tissues. The majority of VHL-null and VHL HIF-1α double-null endothelia (red arrows) is separated from surrounding tissues. Vn, ventricle. Bar, 33 μm.

to develop normally until about E9.5. At E12.5, hemorrhages were found in EC-null embryos (Fig. 1B). The VHL EC-null embryos died at E12.5. At E13.5, no live VHL EC-null embryos were found.

Inactivation of HIF-1α and VHL in EC cannot rescue embryonic lethality. pVHL is a part of an E3 ligase that targets the proteasomal degradation of HIF-α units in the presence of oxygen (26). It has been shown that loss of VHL results in consistent HIF-1α protein expression, which then leads to increased expression of hypoxic response-related genes (19, 24, 32, 43). In VHL patients, tumors are highly vascularized and are known to overproduce VEGF. To understand whether the increased expression of HIF-1α and its downstream target genes plays an important role in the hemorrhage and lethality of VHL EC-null mice, we created VHL$^{+f/+f}$ HIF-1α$^{+f/+f}$ Tie2-Cre (HIF-1α and VHL EC double-null) mice where two floxed

HIF-1α alleles and two floxed VHL alleles were both placed in the background of the Tie2 promoter-driven Cre transgene. By breeding homozygous VHL$^{+f/+f}$ HIF-1α$^{+f/+f}$ female mice and VHL$^{+f/wt}$ HIF-1α$^{+f/+f}$ Tie2-Cre^{+} male mice, we were able to generate VHL$^{+f/+f}$ HIF-1α$^{+f/+f}$ Tie2-Cre^{+} (VHL HIF-1α EC double-null) embryos. Fourteen litters that were generated from this breeding scheme were analyzed from E8.5 to E13.5. The VHL HIF-1α EC double-null mouse embryos died in utero at E12.5. The hemorrhagic phenotype seen in animals lacking HIF-1α and VHL in the endothelium was similar to that seen in those lacking VHL (Fig. 1C). This indicates that loss of HIF-1α did not rescue the embryonic lethality seen in VHL EC-null mice.

It has been reported previously that VHL homozygous null embryos die at E10.5 to E12.5, typically with visible evidence of hemorrhage (18). Our observations indicate that VHL EC-null embryos and VHL HIF-1α EC double-null embryos die at approximately the same stage as global VHL-null embryos, with a grossly similar phenotype.

Endocardium collapse in the hearts of VHL EC-null and VHL HIF-1α EC double-null embryos. Due to hemorrhage found in the hearts of VHL EC-null embryos, heart sagittal sections of wild-type (Fig. 1D), VHL EC-null (Fig. 1E), and VHL HIF-1α EC double-null (Fig. 1F) embryos at E11.5 were analyzed by hematoxylin and eosin staining. In wild-type embryos, elaborate myocardial trabeculae are lined by a layer of well-attached endocardial endothelial cells. Compared with wild-type hearts, the ventricles of EC-null hearts were slightly dilated (data not shown). Although endocardial endothelium can still be visualized within the myocardium at this stage, the collapsed monolayer of EC could be observed in all VHL EC-null and VHL HIF-1α EC double-null embryos.

Loss of VHL in endothelial cells results in abnormal yolk sac vascular organization. The vascularization of yolk sacs in EC-null embryos was also investigated at E11.5. Yolk sac vessels from wild-type embryos displayed differentiated vasculature that is composed of large- and small-diameter vascular branches. These branches formed yolk sac vascular networks (Fig. 1G). Yolk sac vessels of VHL EC-null (Fig. 1H) and VHL HIF-1α EC double-null (Fig. 1I) embryos exhibited different patterns of vascular organization from yolk sac vessels of wild-type embryos: the vascular branches in EC-null embryos were much shorter, and there were few or no vascular networks established between these short branches.

When analyzed by hematoxylin and eosin staining, wild-type endothelium of vitelline vessels maintained tight contact with the surrounding mesoderm and endoderm (Fig. 1J). However, the majority of the vitelline endothelium of VHL EC-null (Fig. 1K) and VHL HIF-1α EC double-null (Fig. 1L) embryos was separated from the surrounding tissues. This indicates that VHL in endothelial cells is required for maintaining yolk sac vascular network integrity.

Defective embryonic vasculogenesis in the placental labyrinth of VHL EC-null and VHL HIF-1α EC double-null mouse embryos at E11.5. A failure of embryonic vasculogenesis in placentas occurs in VHL-null embryos (18). To determine whether EC-null mutant embryos have the same lethal placental developmental defects as homozygous null embryos, placentas from wild-type and EC mutant littermates were analyzed by hematoxylin and eosin staining of the radial sections of whole placentas from E11.5.

In the wild-type placenta, the blood vessels derived from the fetus, which are characterized by nucleated erythrocytes, invade the placental labyrinth and interdigitate with trophoblast-covered maternal blood sinusoids to form densely packed placental labyrinth structures (Fig. 2C and I). In the placentas of VHL homozygous null (VHL$^{-/-}$) embryos (Fig. 2B), three layers of placenta (labyrinth, spongiotrophoblast, and trophoblast giant cell layer) are still discernible. But the volume of null labyrinth was reduced to half the size of the wild-type labyrinth layer (Fig. 2A). The same defects were observed in the placental labyrinth of VHL EC-null (Fig. 2F) and VHL HIF-1α EC double-null (Fig. 2G) embryos compared to wild-type placental labyrinth (Fig. 2E). In the labyrinth of VHL$^{-/-}$ (Fig. 2D), VHL EC-null (Fig. 2J), and VHL HIF-1α EC double-null embryos (Fig. 2K), nucleated erythrocytes were seen only in the portion of the placenta proximal to the embryo. Similar defects were evident at E12.5 in the mutant embryos (data not shown). These abnormalities indicate that VHL EC-null and VHL HIF-1α EC double-null embryos were not able to establish proper embryonic vascular interactions with the maternal circulation; these defects have also been found in homozygous VHL$^{-/-}$ placentas (18).

The Tie2 gene has been shown to be expressed in trophoblastic giant cells (1). This brings up the concern that there may be expression of the Cre transgene, driven by the Tie2 promoter, in trophoblast cells. The placental labyrinths developmental defects could thus result from two possible effects, an inherent defect in the embryonic endothelial cells or a defect in trophoblast differentiation. To distinguish which of these is the primary cause for the defective labyrinth development in mutants, we took advantage of VHL$^{+f/+f}$ conditional mice and Mox2-Cre^{+} transgenic mice to reconstitute VHL-deficient embryos with functionally normal placentas (47). Previous studies have shown that the Cre recombinase gene under the control of an endogenous Mox-2 promoter (Mox2-Cre) is efficiently expressed and functionally active in all cells of E6.5 embryos, with no expression in the trophoblast or extraembryonic endoderm lineages. By breeding VHL$^{+f/wt}$ Mox2-Cre^{+} male mice with homozygous VHL$^{+f/+f}$ conditional mice, we were able to generate VHL$^{+f/+f}$ Mox2-Cre^{+} embryos, which are VHL-deficient embryos with intact extraembryonic tissues. By this mating scheme, 25% of live born pups should be of the VHL$^{+f/+f}$ Mox2-Cre-positive genotype, if the embryonic lethality of VHL$^{+f/+f}$ Tie2-Cre mice is rescued by the wild-type genotype placentas.

Fourteen litters of mice from this mating cross were screened after birth, and no VHL$^{+f/+f}$ Mox2-Cre-positive mice were found. Seven litters from the same breeding scheme were analyzed from E10.5 to E13.5. VHL$^{+f/+f}$ Mox2-Cre-positive mice died in utero at E12.5 with a hemorrhage phenotype similar to that seen with VHL EC-null mice (data not shown). The placental development of VHL$^{+f/+f}$ Mox2-Cre-positive mice was also analyzed by hematoxylin and eosin staining. As shown in Fig. 2H and L, the placentas of VHL$^{+f/+f}$ Mox2-Cre-positive embryos demonstrated the same phenotypic defects as the placentas of VHL EC-null embryos. This indicates that wild-type placentas cannot rescue the embryonic lethality and de-

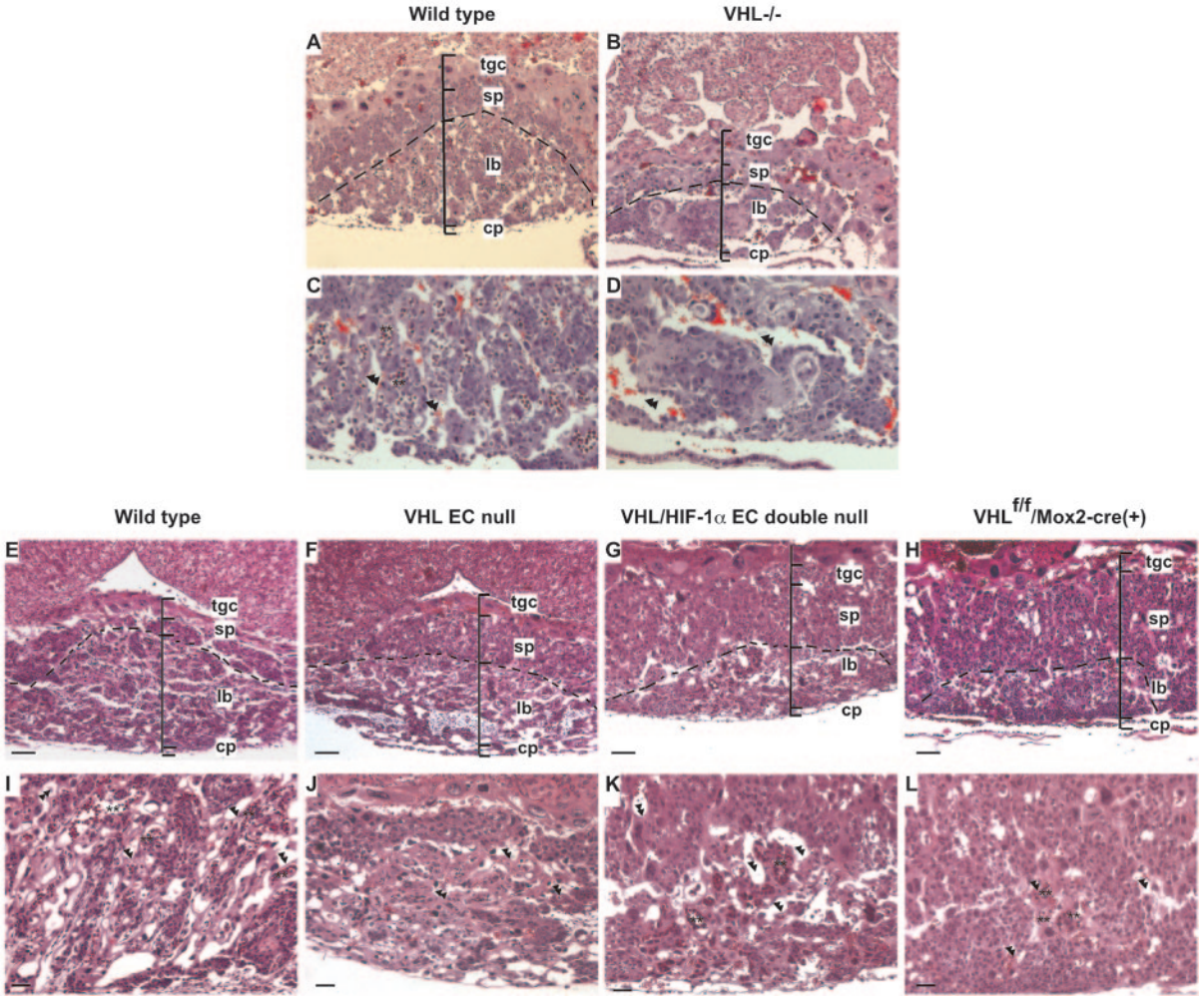

FIG. 2. Embryonic vasculogenesis is defective in placental labyrinth of VHL EC-null and VHL HIF-1α EC double-null embryos. (A and B) H&E staining of the placental radial sections prepared from wild-type (A) and $VHL^{-/-}$ (B) littermates at E11.5. The volume of labyrinth of null placenta (B) is almost a half size smaller than the volume of labyrinth of wild-type placenta (A). tgc, trophoblastic giant cells; sp, spongiotrophoblast; lb, labyrinth, cp, chorionic plate. (C and D) The higher-power magnification of the H&E-stained sections shows the structure of the placental labyrinth from wild-type (C) and $VHL^{-/-}$ (D) mouse embryos at E11.5. Asterisks and arrowheads indicate fetal blood spaces and maternal blood spaces, respectively. (E to H) H&E staining of the placental radial sections prepared from wild-type (E), VHL EC-null (F), VHL HIF-1α EC double-null (G), and $VHL^{+f/+f}$ Mox2-Cre^{+} (H) embryos at E11.5. The volume of labyrinth of mutant embryos (F to H) is almost a half size smaller than the volume of labyrinth of wild-type embryos (E). Abbreviations are the same as those defined for panels A to D. Bar, 100 μm. (I to L) The higher-power magnification of the H&E-stained sections shows the structure of the placental labyrinth from wild-type (I), VHL EC-null (J), VHL HIF-1α EC double-null (K), and $VHL^{+f/+f}$ Mox2-Cre^{+} (L) embryos at E11.5. In the placental labyrinth of wild-type embryos (I), the fetal vessels containing nucleated erythrocytes interdigitate with the maternal blood sinuses containing nonnucleated erythrocytes to form a nice labyrinth network. In the placental labyrinth of mutant embryos (J to L), maternal blood sinuses are predominantly saturated; the fetal vessels are only on the edge of embryo side of the labyrinth and have not invaded to the labyrinth. Asterisks and arrowheads indicate fetal blood spaces and maternal blood spaces, respectively. (C and I) Arrowheads, trophoblast-covered maternal blood sinusoids. Bar, 50 μm.

fective labyrinth of VHL EC-null mice. This also indicates that the defective embryonic vasculogenesis within the placental labyrinth of the VHL homozygous null embryos is due to the loss of VHL in embryonic endothelial cells.

Dilated vessels and reduced vessel complexity in VHL EC-null and VHL HIF-1α EC double-null mouse embryos. To determine the effects of the mutation on embryonic vessel development, whole-mount vessel staining of yolk sacs and embryos in wild-type, VHL-null, and EC-null littermates at E11.5 was investigated, using antibodies against the endothelial cell marker CD31. Abnormally dilated vitelline vessels and decreased vessel complexity were observed in the yolk sacs of both VHL-null and EC-null embryos (Fig. 3D, F, and G) compared with the vascular patterning in wild-type yolk sacs (Fig. 3C and E). The vessels in the heads of the VHL-null (Fig. 3B), VHL EC-null (Fig. 3I), and VHL HIF-1α EC-null (Fig. 3J) mutant embryos were greatly dilated compared to wild-type littermates (Fig. 3D). The complexity of the vascular network of the cephalic and dorsal regions was also reduced in the mutant embryos (Fig. 3I, J, L, and M) compared to wild-type embryos (Fig. 3A and H). Similar vascular network defects were observed at E10.5 in the mutant embryos (data not shown). These results indicate that VHL in embryonic endothelium plays a key role in regulating vessel morphology.

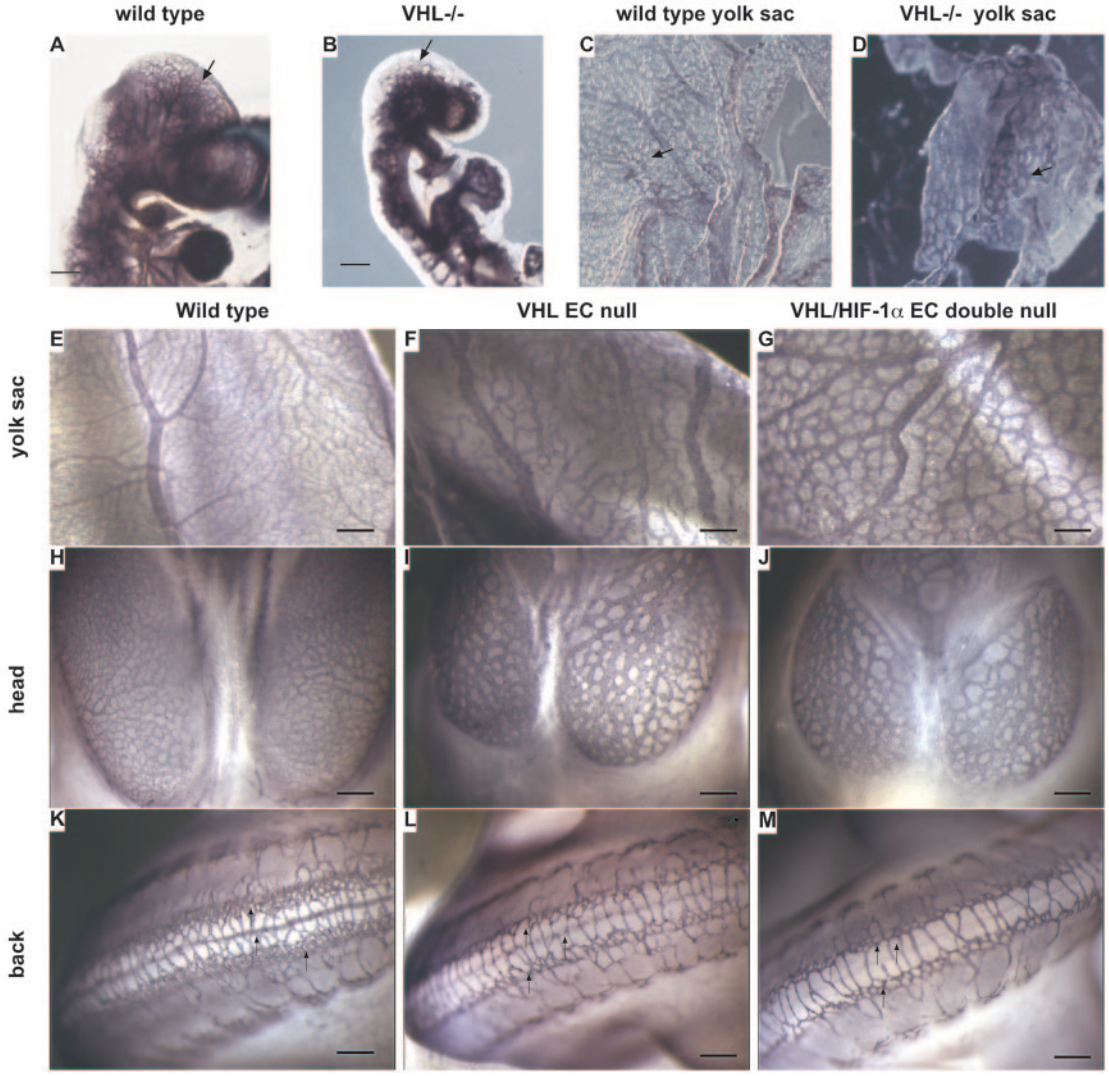

FIG. 3. Dilated vessels and reduced vessel complexity in VHL EC-null and VHL HIF-1α EC double-null embryos. (A and B) Whole-mount CD31 staining displays the vessels of $VHL^{-/-}$ embryos (B), which are much more dilated than those of wild-type embryos (A). (C and D) Whole-mount CD31 staining displays the vessel network structure of yolk sacs from wild-type (C) and $VHL^{-/-}$ (D) embryos at E11.5. Black arrows indicate the vessels. (E to G) Whole-mount CD31 staining of yolk sacs from wild-type (E), VHL EC-null (F), and VHL HIF-1α EC double-null (G) embryos at E11.5. Bar, 200 μm. (H to J) Whole-mount CD 31 staining displays the endothelial cells of the vessels in the heads of the wild-type (H), VHL EC-null (I), and VHL HIF-1α EC double-null (J) embryos at E11.5. The vessels in the heads of null embryos display dilated vessels and decreased vessel complexity, compared to the vessels of wild-type embryos. Bar, 200 μm. (K to M) Whole-mount CD31 staining displays the vessels on the backs of wild-type (K), VHL EC-null (L), and VHL HIF-1α EC double-null (M) embryos at E11.5. The complexity of the vessel network dramatically decreased in null embryos compared with wild-type controls. Black arrows indicate the capillary network. Bar, 200 μm.

Hypoxic response-related genes expression in VHL-null and VHL-null/HIF-1α-null ECs. Previous studies have shown that loss of VHL causes increased expression of HIF-1-regulated genes, including VEGF, GLUT-1, and PGK. However, eNOS and Tie2 have been reported to be regulated by the HIF-2α transcription factor (8, 11, 49). To determine the specificity of endothelial expression of HIF-1 genes, lung microvascular ECs were isolated from $VHL^{+f/+f}$ or $VHL^{+f/+f}$ HIF-$1\alpha^{+f/+f}$ mice. The mRNA expression level of these genes was compared in VHL HIF-1α wild-type ECs ($VHL^{+f/+f}$ HIF-$1\alpha^{+f/+f}$ ECs infected with adenovirus expressing β-galactosidase as a control for viral infection), $VHL^{-/-}$ ECs ($VHL^{+f/+f}$ ECs infected with adenovirus expressing Cre recombinase), and $VHL^{-/-}$ HIF-$1\alpha^{-/-}$ ECs ($VHL^{+f/+f}$ HIF-$1\alpha^{+f/+f}$ ECs infected with adenovirus expressing Cre recombinase); ECs were cultured at normoxia or hypoxia. Relative to the robust induction of VEGF, GLUT-1, PGK, and iNOS in both wild-type and $VHL^{-/-}$ cells at hypoxia, there was only a moderate induction of these genes in $VHL^{-/-}$ ECs under normoxic conditions (Fig. 4A to D). In VHL-null HIF-1α-null ECs, the hypoxic induction of VEGF, GLUT-1, PGK, and iNOS genes was almost abolished. The expression of Ang-1, Ang-2, eNOS, and Tie2 was not significantly different between wild-type, VHL-null, and VHL-null HIF-1α-null ECs under either normoxic or hypoxic conditions (Fig. 4E to H). The results here further confirm previous findings, indicating that HIF-1α

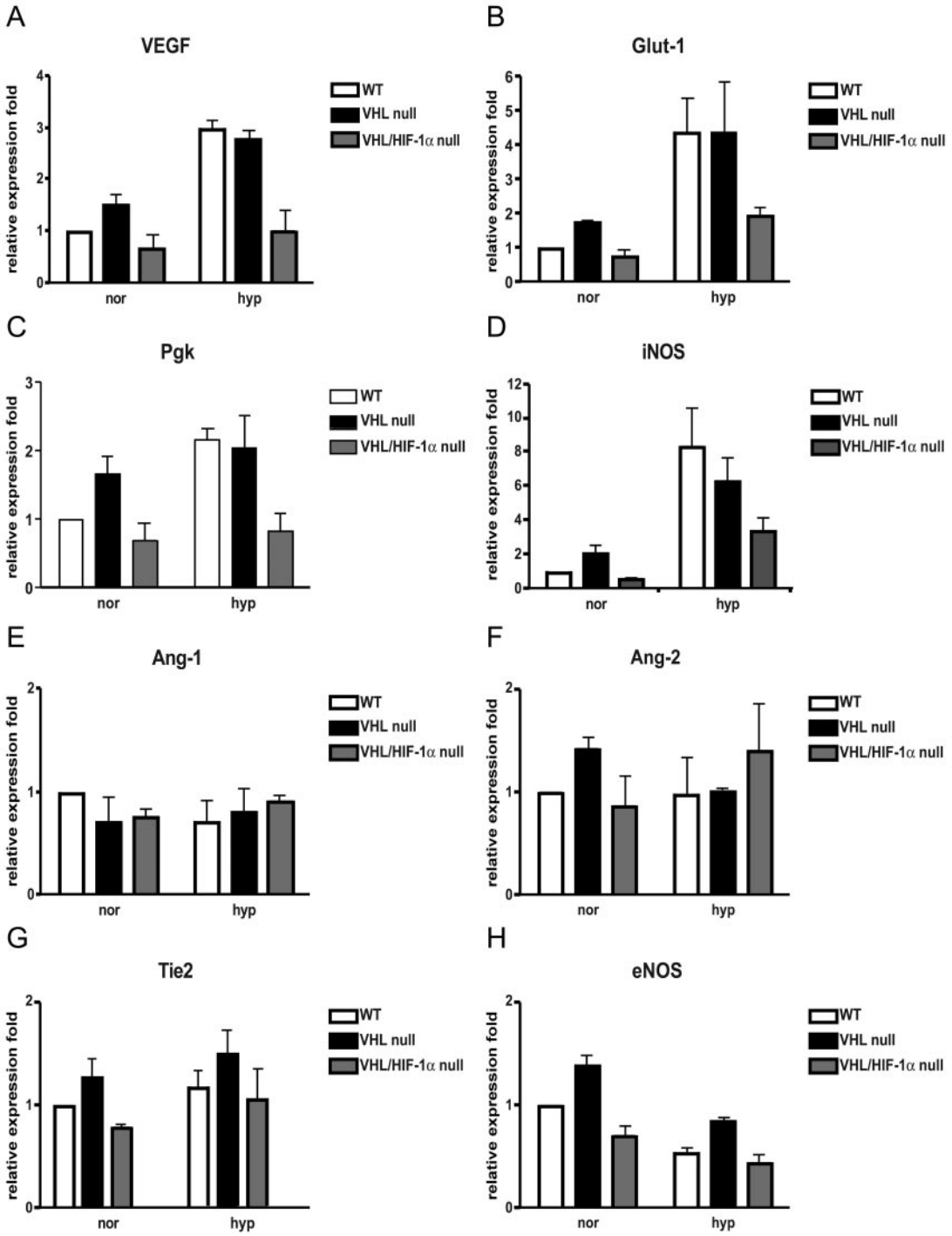

FIG. 4. Hypoxic response-related gene expression in VHL$^{-/-}$ and VHL$^{-/-}$ HIF-1α$^{-/-}$ ECs. Purified wild-type ECs (white bars), VHL$^{-/-}$ ECs (black bars), and VHL$^{-/-}$ HIF-1α$^{-/-}$ ECs (gray bars) were cultured under normoxic (20% oxygen) or hypoxic (0.5% oxygen) conditions for 8 h; total RNA was isolated and expression of target genes was determined by real-time PCR. Values were normalized to real-time PCR results for rRNA. After normalization, the relative expression of each gene was expressed as a percentage of that observed with wild-type cells at normoxia (mean ± standard deviation).

is the primary transcription factor regulating the endothelial cell hypoxic response (48).

Reduced fibronectin deposition around vitelline vessels of yolk sacs from VHL EC-null and VHL HIF-1α EC double-null mouse embryos. Fibronectin and fibronectin receptor α5 are critical for proper yolk sac vessel organization and for the maintenance of the contact points of vitelline endothelium with surrounding yolk sac tissues (15, 16). The vascular defects of VHL EC-null yolk sacs are similar in many regards to the defects found in yolk sacs of FN-null and α5-null mutant embryos.

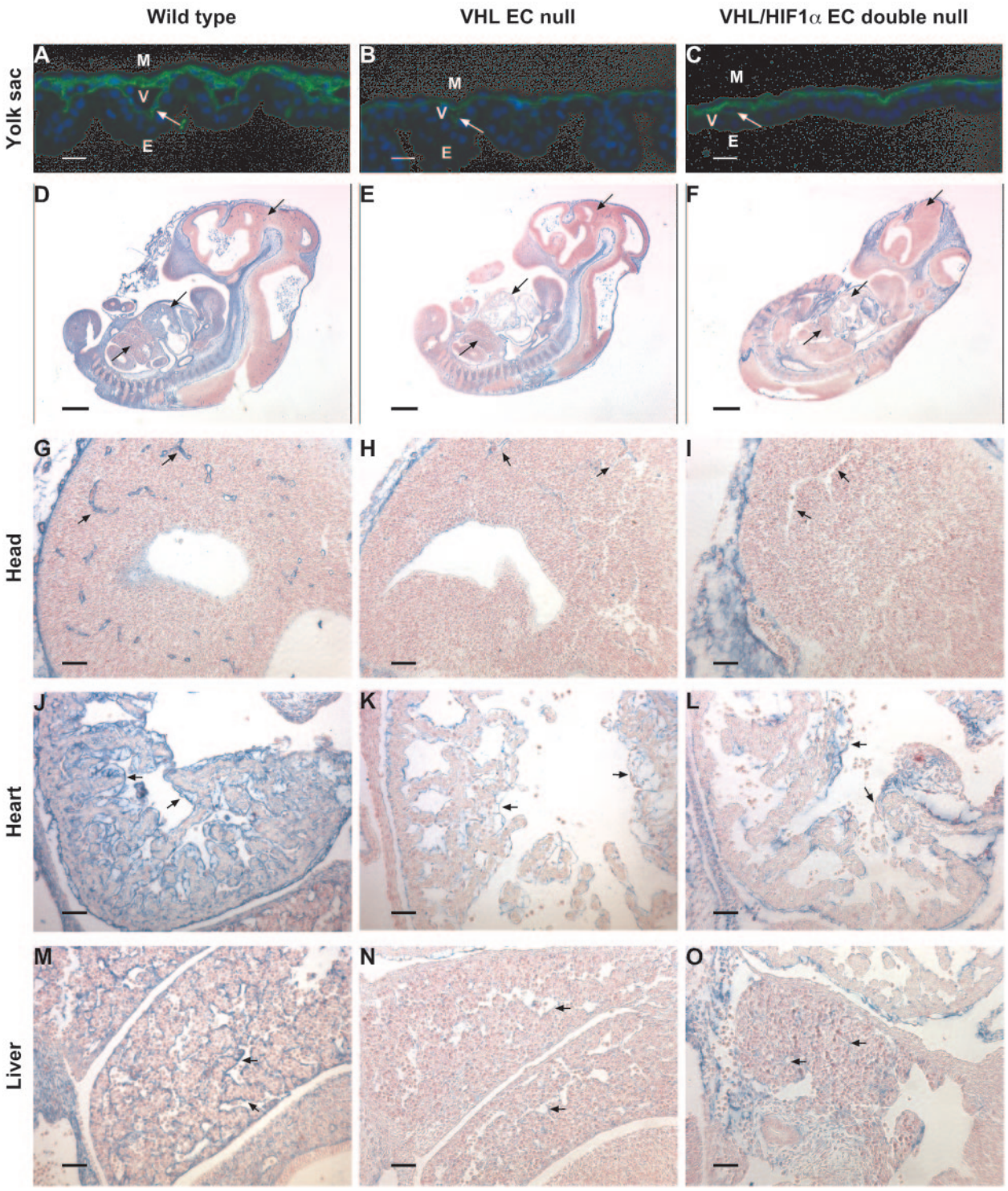

FIG. 5. Diminished fibronectin staining around vessels in VHL EC-null and VHL HIF-1α EC double-null mouse embryos. (A to C) Fibronectin (green color) fluorescence staining of yolk sac sections of wild-type (A), VHL EC-null (B), and VHL HIF-1α EC double-null (C) embryos at E11.5. The fibronectin linear staining at the endoderm-endothelial basement membrane interface is greatly reduced in yolk sacs from both VHL EC-null (E) and VHL HIF-1α EC double-null (F) embryos. White arrows indicate the endoderm-endothelial interface. M, mesodermal layer of cells; E, endodermal layer of cells; V, vitelline blood vessels. Bar, 100 μm. (D to F) Sagittal sections of wild-type (D), VHL EC-null (E), and VHL HIF-1α EC double-null (F) mouse embryos at E11.5 were stained with antifibronectin antisera (blue color). The counterstain was Vector Red. Black arrows indicate the comparable regions that are shown in panels G to O. Bar, 500 μm. (G to I) Higher-power-magnification views of comparable regions of heads. The fine linear fibronectin staining was specifically detected on the vessels of wild-type embryos (G), and vessel fibronectin staining was almost diminished in VHL EC-null (H) and VHL HIF-1α EC double-null (I) embryos. Black arrows indicate the vessels. Bar, 50 μm. (J to L) Higher-power-magnification views of comparable regions of hearts. The specific fibronectin staining was detected only on the endocardial layer of the heart of wild-type embryos (J), and endocardial fibronectin staining was almost absent in VHL EC-null (K) and VHL HIF-1α EC double-null (L) embryos. Black arrows indicate the endocardial endothelial layer. Bar, 50 μm. (M to O) Higher-power-magnification views of comparable regions of livers. Specific fibronectin staining is only on the vessels of wild-type embryos (M), and linear fibronectin staining around vessels was almost absent in VHL EC-null (N) and VHL HIF-1α EC double-null (O) embryos. Black arrows indicate the vessels. Bar, 50 μm.

We investigated the fibronectin expression of wild-type, VHL EC-null, and VHL HIF-1α EC double-null yolk sacs by fibronectin immunofluorescence staining. The fibronectin deposition around vitelline vessels, in particular at the endoderm-endothelial basement membrane interface, was greatly reduced in yolk sacs from both VHL EC-null (Fig. 5B) and VHL HIF-1α EC double-null (Fig. 5C) mutant embryos. This indicates that vascular defects in the VHL EC-null yolk sac are coincident with defects in fibronectin deposition around vitelline endothelium.

Diminished fibronectin deposition around endothelia of VHL EC-null and VHL EC HIF-1α double-null mouse embryos. We further compared fibronectin expression levels in the embryonic endothelium by immunostaining. The sagittal sections of embryos at E11.5 at comparable regions are shown in Fig. 5D to O: fibronectin expression was mainly detected within head mesenchyme, notochord, somites, and the endocardium and vessels of the embryos, as previously reported (17). Higher-power magnification clearly shows specific endothelial fibronectin staining only in the vessels of the heads and livers and in the endocardial endothelial cell layer of the heart (Fig. 5G to O). The fibronectin staining in the endothelium was highly reduced by the loss of VHL in ECs (Fig. 5H, I, K, L, N, and O), whereas fibronectin expression in the notochord and somites was equally strong in wild-type and EC-null mice. This finding is consistent with previous studies of $VHL^{-/-}$ embryos (37). This indicates that endothelial VHL is critical for depositing and maintaining fibronectin in embryonic vessels and in endocardial endothelium.

Defective extracellular fibronectin matrix assembly by VHL-null and VHL-null HIF-1α-null EC. Fibronectin has been shown to directly bind with pVHL in vivo, and the extracellular fibronectin assembly is defective in cells lacking pVHL (37). After culture of wild-type, $VHL^{-/-}$, and VHL-null HIF-1α-null ECs in fibronectin-depleted medium for 1 week, we detected fibronectin by indirect immunofluorescence staining using antifibronectin antisera. Consistent with previous studies of renal carcinoma cells and $VHL^{-/-}$ mouse embryonic fibroblasts (37), it was found that assembly of normal extracellular fibronectin was greatly reduced in both $VHL^{-/-}$ and VHL-null HIF-1α-null ECs. Wild-type ECs can produce abundant extracellular fibronectin fibrils that are characterized by stretched fiber-like structures outside of the EC (Fig. 6A). But these extracellular fibronectin fibrils were greatly reduced in both $VHL^{-/-}$ (Fig. 6B) and VHL-null HIF-1α-null (Fig. 6C) ECs. This indicates that less fibronectin is deposited/retained in the extracellular matrix of $VHL^{-/-}$ ECs and VHL-null HIF-1α-null ECs.

Loss of VHL increases the permeability of the endothelial monolayer. Endothelial monolayer integrity is influenced by cell-matrix interactions. The extracellular matrix plays a central role in maintaining vascular integrity by a connection with the cell matrix and cytoskeleton (9, 25, 50). The defective extracellular fibronectin assembly in VHL-deficient endothelial cells prompted us to investigate if VHL played a functional role in maintaining the integrity of endothelial cells. We compared the paracellular permeability of $VHL^{-/-}$ and $VHL^{-/-}$ HIF-$1\alpha^{-/-}$ ECs to wild-type ECs. Both $VHL^{-/-}$ and $VHL^{-/-}$ HIF-$1\alpha^{-/-}$ ECs were more permeable to high-molecular-weight dextran than wild-type ECs (Fig. 6D).

Both $VHL^{-/-}$ and $VHL^{-/-}$ HIF-$1\alpha^{-/-}$ ECs display impaired migration. The extracellular matrix plays a determining role in controlling cell migration (22, 28). We sought to evaluate the effect of VHL deletion on endothelial cell migration. We compared the migration of wild-type, $VHL^{-/-}$, and $VHL^{-/-}$ HIF-$1\alpha^{-/-}$ ECs through either a fibronectin-coated or a collagen-coated Boyden chamber. As shown in Fig. 6E, the motility of both $VHL^{-/-}$ and VHL-null HIF-1α-null ECs was greatly reduced compared to wild-type ECs, regardless of the coating on transwells. The motility of both wild-type and VHL-null ECs was significantly increased by fibronectin coating, but the fibronectin-increased migration was greater in $VHL^{-/-}$ and VHL-null HIF-1α-null ECs (3.7- to 4.3-fold difference) compared to wild type ECs (2.1-fold difference).

Impaired adhesion of $VHL^{-/-}$ and VHL-null HIF-1α-null ECs can be partially rescued by exogenous FN. The assembly of fibronectin is very important for EC initial adhesion, and defects in fibronectin assembly can affect vessel maturation (39, 41). We investigated the adhesion of $VHL^{-/-}$ and VHL-null HIF-1α-null ECs in the presence and absence of fibronectin in vitro. We cultured wild-type and mutant ECs in fibronectin-free culture medium for 1 week. Then, we tested the adhesion capacity of wild-type and VHL-null ECs on uncoated culture plates or plates coated with fibronectin. VHL-null ECs showed >7-fold-reduced adhesion on normal surfaces compared to wild-type ECs (Fig. 5G). But the fibronectin coating partially rescued the impaired adhesion of VHL-null ECs, reducing the differential adhesion to only 1.7 fold compared to wild-type ECs in the presence of the factor.

DISCUSSION

Previous studies established the essential roles of HIF and VHL during placental labyrinth development (2, 18). It has been shown that VHL-nullizygous embryos ($VHL^{-/-}$) die in utero between E10.5 and E12.5, due to the absence of placental embryonic vasculogenesis and to subsequent hemorrhage and necrosis. The placental defects of VHL-null embryos are thought to be linked to decreased VEGF expression in $VHL^{-/-}$ trophoblasts.

We have shown that the proper function of pVHL in ECs is essential for the development of intraembryonic and extraembryonic endothelia. Interestingly, $VHL^{+f/+f}$ Tie2-Cre embryos die at E12.5 with embryonic vasculogenic defects in the placental labyrinth, which are similar to those seen with $VHL^{-/-}$ mice. We have also shown that genetically wild-type placentas cannot rescue the embryonic lethality of VHL-null mice. This indicates that endothelium is the primary tissue affected by loss of VHL during embryonic development. The loss of VHL function in EC causes the developmental failure of embryonic vasculogenesis in the placental labyrinth.

VHL has been identified as a tumor suppressor, and VHL-associated tumors are typically hypervascular, with high levels of expression of VEGF. Previous studies have already demonstrated that pVHL-defective cells fail to downregulate HIF-α subunits (19, 24, 32, 33, 43). To understand the role of HIF-1α in defective placental development of VHL-null mice, we generated VHL HIF-1α conditional double-null mice and found that deletion of HIF-1α in VHL-null endothelial cells could not rescue the embryonic lethality and developmental defects

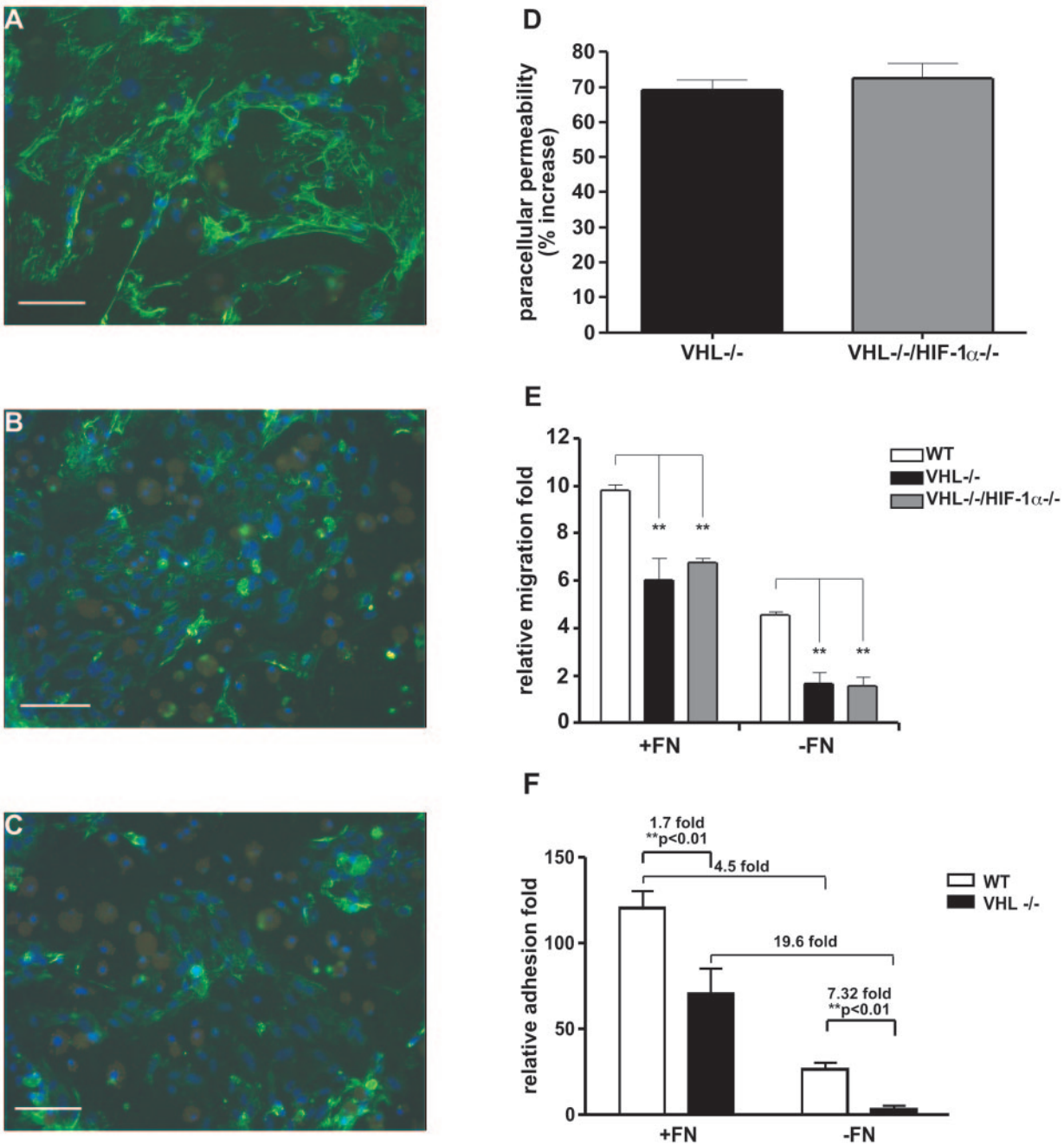

FIG. 6. Defective extracellular fibronectin matrix assembly by VHL$^{-/-}$ and VHL-null HIF-1α-null ECs. (A to C) Wild-type (A), VHL$^{-/-}$ (B), and VHL$^{-/-}$ HIF-1α$^{-/-}$ (C) ECs were grown on coverslides in fibronectin-depleted medium for 1 week. Fibronectin (green color) was detected by indirect immunofluorescence staining using polyclonal antifibronectin antisera. Cell numbers were visualized with DAPI staining (blue color). Both VHL$^{-/-}$ (B) and VHL$^{-/-}$ HIF-1α$^{-/-}$ (C) ECs assemble very few fibronectin fibrils compared to wild-type ECs (A). Bar, 100 μm. (D) Permeability across the EC monolayer. VHL$^{-/-}$ (black bar) and VHL$^{-/-}$ HIF-1α$^{-/-}$ (gray bar) confluent ECs show a >70% increased passage of FITC-dextran compared with wild-type ECs (mean ± SEM). (E) Migration of ECs was analyzed in a Boyden chamber. Wild-type (white bars), VHL$^{-/-}$ (black bars), and VHL$^{-/-}$ HIF-1α$^{-/-}$ (gray bars) ECs were plated in transwells either coated with fibronectin (+FN) or coated with collagen (−FN). The migrating cells were stained as described in Materials and Methods (results are shown as the mean ± SEM). (F) Adhesion assay. Forty-eight-well plates were coated with either 5-μg/well fibronectin (+FN) or PBS (−FN). A total of 5×10^4 EC in 200 μl serum-free adhesion medium were plated in the wells and allowed to attach for 1 h. Wild-type ECs (white bars) and VHL-null ECs (black bars) were then washed gently, and the adherent cells were stained with 0.1% crystal violet solution. The dye was dissolved in methanol, and the absorbance of the solution was read at 595 nm in an enzyme-linked immunosorbent assay plate reader (mean ± SEM). Statistical analysis was performed using the unpaired Student's test. *, $P < 0.05$; **, $P < 0.01$.

of embryonic endothelium caused by the absence of VHL. Gene expression analysis demonstrates that loss of HIF-1α is sufficient to block hypoxia-inducible gene expression in $VHL^{-/-}$ ECs. This is in agreement with our previous finding that HIF-1α is the primary transcription factor regulating hypoxic gene induction in endothelial cells (48). These gene expression results further suggest that placental and vascular developmental defects of VHL EC-null embryos are independent of regulation of HIF-1α and HIF-1α-induced genes.

VHL has been shown to be important for extracellular FN matrix assembly (37). Cells lacking pVHL secrete FN but are defective in FN matrix assembly, and an FN assembly defect can be observed in all disease-associated pVHL mutations examined to date (36). A recent study has found that a pVHL mutant, which retains its ability for HIF regulation but fails to assemble fibronectin matrix, does not suppress tumor growth (46). This indicates a potential key role of defective fibronectin assembly in VHL disease.

FN is the earliest and most abundantly expressed matrix molecule during embryonic vascular development. During the formation of endothelial tubes, FN is abundant in the mesenchyme and persists throughout adult life in the basement membrane surrounding blood vessels (17). FN nullizygous ($FN^{-/-}$) embryos initially develop normally, but by embryonic day 8 they begin to develop defects in the neural tube and in mesodermally derived tissues. After day 8.5, failure in the development of both embryonic and extraembryonic vasculature is the likely cause of death of fibronectin-null mutant embryos (16). A lineage analysis demonstrated that FN-null endothelial cells form dilated vessels and fail to either establish or maintain contact with the surrounding mesenchyme (16). The vasculogenesis defects that were observed in FN-null embryos demonstrate that FNs are essential for attachment and/or maintenance of the endothelium in contact with mesoderm and yolk sac blood vessel formation. The high level of expression of FN in embryonic endothelium in placental labyrinth also indicates its important role in the development of placental labyrinth (44). A number of studies have confirmed this essential role of extracellular FN assembly in ECs during vascular development (15, 22, 23), which indicates that endothelial cells play an active role in organizing and assembling the FN matrix and that the failure to organize the matrix appropriately in the endothelial cell basement membrane could lead to defective endothelial cell adhesion and migration and hence to defects in vessel remodeling and angiogenesis.

In this paper, we have shown that loss of VHL in endothelial cells leads to defective assembly of extracellular FN matrix in an HIF-1α-independent fashion. By immunostaining, we have found that fibronectin is only expressed in the vessels of the heads and liver and in the endocardial endothelial cell layer of the heart. Linear deposits of FN in vessel basement membranes are totally absent in VHL EC-null and VHL/HIF-1α EC-null embryos. The phenotypic defects that we observed with VHL EC-null and VHL HIF-1α EC-null embryos are similar to the developmental defects seen with $FN^{-/-}$ embryos, including dilated vessels and abnormal extraembryonic vasculature (16). This suggests that VHL regulation of fibronectin deposition in vessel basement membranes plays a key functional role in embryonic vascularization.

The extracellular matrix in vessel basement membranes plays a central role in vessel integrity (4, 12, 25). Here, we have found that both $VHL^{-/-}$ and VHL-null HIF-1α-null ECs are more permeable to high-molecular-weight dextran than wild-type ECs. This defective functional integrity would explain the presence of vascular leakage and hemorrhages in EC-null embryos. This also supports the hypothesis that the functional defects of $VHL^{-/-}$ ECs are likely extracellular fibronectin dependent and HIF-1α independent. Furthermore, we have shown that the adhesive ability and motility of $VHL^{-/-}$ EC is dramatically decreased relative to wild-type endothelial cells and that these defects can be partially rescued by exogenous fibronectin. Thus, these data indicate that the vascular developmental defects of VHL-null, VHL EC-null, and VHL HIF-1α EC-null embryos are caused by abnormal endothelial fibronectin assembly. Endothelial cells require VHL for correct vascular patterning and maintenance of vascular integrity at the middle stages of development.

It has been found that an intact HIF pathway in the absence of proper fibronectin matix assembly is insufficient to suppress tumor formation (46). In our study, we have further demonstrated that outside of its function in regulating hypoxic response, VHL plays a key role in establishing the structure of extracellular matrix during vascular development. This clearly demonstrates that pVHL-dependent regulation of fibronectin assembly, independent of VHL function in regulating HIF-1α, plays an essential role during early vessel development.

REFERENCES

1. **Abbott, B. D., and A. R. Buckalew.** 2000. Placental defects in ARNT-knockout conceptus correlate with localized decreases in VEGF-R2, Ang-1, and Tie-2. Dev. Dyn. **219:**526–538.
2. **Adelman, D. M., M. Gertsenstein, A. Nagy, M. C. Simon, and E. Maltepe.** 2000. Placental cell fates are regulated in vivo by HIF-mediated hypoxia responses. Genes Dev. **14:**3191–3203.
3. **Adryan, B., H. J. Decker, T. S. Papas, and T. Hsu.** 2000. Tracheal development and the von Hippel-Lindau tumor suppressor homolog in Drosophila. Oncogene **19:**2803–2811.
4. **Alexander, J. S., and J. W. Elrod.** 2002. Extracellular matrix, junctional integrity and matrix metalloproteinase interactions in endothelial permeability regulation. J. Anat. **200:**561–574.
5. **Bishop, T., K. W. Lau, A. C. Epstein, S. K. Kim, M. Jiang, D. O'Rourke, C. W. Pugh, J. M. Gleadle, M. S. Taylor, J. Hodgkin, and P. J. Ratcliffe.** 2004. Genetic analysis of pathways regulated by the von Hippel-Lindau tumor suppressor in Caenorhabditis elegans. PLoS Biol. **2:**e289.
6. **Bruick, R. K., and S. L. McKnight.** 2001. A conserved family of prolyl-4-hydroxylases that modify HIF. Science **294:**1337–1340.
7. **Cohen, H. T., M. Zhou, A. M. Welsh, S. Zarghamee, H. Scholz, D. Mukhopadhyay, T. Kishida, B. Zbar, B. Knebelmann, and V. P. Sukhatme.** 1999. An important von Hippel-Lindau tumor suppressor domain mediates Sp1-binding and self-association. Biochem. Biophys. Res. Commun. **266:**43–50.
8. **Coulet, F., S. Nadaud, M. Agrapart, and F. Soubrier.** 2003. Identification of hypoxia-response element in the human endothelial nitric-oxide synthase gene promoter. J. Biol. Chem. **278:**46230–46240.
9. **Defilippi, P., C. Olivo, M. Venturino, L. Dolce, L. Silengo, and G. Tarone.** 1999. Actin cytoskeleton organization in response to integrin-mediated adhesion. Microsc. Res. Tech. **47:**67–78.
10. **Duan, D. R., A. Pause, W. H. Burgess, T. Aso, D. Y. Chen, K. P. Garrett, R. C. Conaway, J. W. Conaway, W. M. Linehan, and R. D. Klausner.** 1995. Inhibition of transcription elongation by the VHL tumor suppressor protein. Science **269:**1402–1406.
11. **Duan, L. J., Y. Zhang-Benoit, and G. H. Fong.** 2005. Endothelium-intrinsic requirement for Hif-2α during vascular development. Circulation **111:**2227–2232.
12. **Engbring, J. A., and H. K. Kleinman.** 2003. The basement membrane matrix in malignancy. J. Pathol. **200:**465–470.
13. **Epstein, A. C., J. M. Gleadle, L. A. McNeill, K. S. Hewitson, J. O'Rourke, D. R. Mole, M. Mukherji, E. Metzen, M. I. Wilson, A. Dhanda, Y. M. Tian, N. Masson, D. L. Hamilton, P. Jaakkola, R. Barstead, J. Hodgkin, P. H. Maxwell, C. W. Pugh, C. J. Schofield, and P. J. Ratcliffe.** 2001. C. elegans EGL-9 and mammalian homologs define a family of dioxygenases that regulate HIF by prolyl hydroxylation. Cell **107:**43–54.
14. **Esteban-Barragan, M. A., P. Avila, M. Alvarez-Tejado, M. D. Gutierrez, A.**

Garcia-Pardo, F. Sanchez-Madrid, and M. O. Landazuri. 2002. Role of the von Hippel-Lindau tumor suppressor gene in the formation of beta1-integrin fibrillar adhesions. Cancer Res. **62:**2929–2936.
15. **Francis, S. E., K. L. Goh, K. Hodivala-Dilke, B. L. Bader, M. Stark, D. Davidson, and R. O. Hynes.** 2002. Central roles of α5β1 integrin and fibronectin in vascular development in mouse embryos and embryoid bodies. Arterioscler. Thromb. Vasc. Biol. **22:**927–933.
16. **George, E. L., H. S. Baldwin, and R. O. Hynes.** 1997. Fibronectins are essential for heart and blood vessel morphogenesis but are dispensable for initial specification of precursor cells. Blood **90:**3073–3081.
17. **George, E. L., E. N. Georges-Labouesse, R. S. Patel-King, H. Rayburn, and R. O. Hynes.** 1993. Defects in mesoderm, neural tube and vascular development in mouse embryos lacking fibronectin. Development **119:**1079–1091.
18. **Gnarra, J. R., J. M. Ward, F. D. Porter, J. R. Wagner, D. E. Devor, A. Grinberg, M. R. Emmert-Buck, H. Westphal, R. D. Klausner, and W. M. Linehan.** 1997. Defective placental vasculogenesis causes embryonic lethality in VHL-deficient mice. Proc. Natl. Acad. Sci. USA **94:**9102–9107.
19. **Gnarra, J. R., S. Zhou, M. J. Merrill, J. R. Wagner, A. Krumm, E. Papavassiliou, E. H. Oldfield, R. D. Klausner, and W. M. Linehan.** 1996. Post-transcriptional regulation of vascular endothelial growth factor mRNA by the product of the VHL tumor suppressor gene. Proc. Natl. Acad. Sci. USA **93:**10589–10594.
20. **Haas, T. L., and J. A. Madri.** 1999. Extracellular matrix-driven matrix metalloproteinase production in endothelial cells: implications for angiogenesis. Trends Cardiovasc. Med. **9:**70–77.
21. **Haase, V. H., J. N. Glickman, M. Socolovsky, and R. Jaenisch.** 2001. Vascular tumors in livers with targeted inactivation of the von Hippel-Lindau tumor suppressor. Proc. Natl. Acad. Sci. USA **98:**1583–1588.
22. **Ilic, D., B. Kovacic, K. Johkura, D. D. Schlaepfer, N. Tomasevic, Q. Han, J. B. Kim, K. Howerton, C. Baumbusch, N. Ogiwara, D. N. Streblow, J. A. Nelson, P. Dazin, Y. Shino, K. Sasaki, and C. H. Damsky.** 2004. FAK promotes organization of fibronectin matrix and fibrillar adhesions. J. Cell Sci. **117:**177–187.
23. **Ilic, D., B. Kovacic, S. McDonagh, F. Jin, C. Baumbusch, D. G. Gardner, and C. H. Damsky.** 2003. Focal adhesion kinase is required for blood vessel morphogenesis. Circ. Res. **92:**300–307.
24. **Iliopoulos, O., A. P. Levy, C. Jiang, W. G. Kaelin, Jr., and M. A. Goldberg.** 1996. Negative regulation of hypoxia-inducible genes by the von Hippel-Lindau protein. Proc. Natl. Acad. Sci. USA **93:**10595–10599.
25. **Jain, R. K.** 2003. Molecular regulation of vessel maturation. Nat. Med. **9:**685–693.
26. **Kaelin, W. G., Jr.** 2002. Molecular basis of the VHL hereditary cancer syndrome. Nat. Rev. Cancer **2:**673–682.
27. **Kaelin, W. G., Jr.** 2004. The von Hippel-Lindau tumor suppressor gene and kidney cancer. Clin. Cancer Res. **10:**6290S–5S.
28. **Kalluri, R.** 2003. Basement membranes: structure, assembly and role in tumour angiogenesis. Nat. Rev. Cancer **3:**422–433.
29. **Kibel, A., O. Iliopoulos, J. A. DeCaprio, and W. G. Kaelin, Jr.** 1995. Binding of the von Hippel-Lindau tumor suppressor protein to elongin B and C. Science **269:**1444–1446.
30. **Kisanuki, Y. Y., R. E. Hammer, J. Miyazaki, S. C. Williams, J. A. Richardson, and M. Yanagisawa.** 2001. Tie2-Cre transgenic mice: a new model for endothelial cell-lineage analysis in vivo. Dev. Biol. **230:**230–242.
31. **Mack, F. A., W. K. Rathmell, A. M. Arsham, J. Gnarra, B. Keith, and M. C. Simon.** 2003. Loss of pVHL is sufficient to cause HIF dysregulation in primary cells but does not promote tumor growth. Cancer Cell **3:**75–88.
32. **Maher, E. R., and W. G. Kaelin, Jr.** 1997. von Hippel-Lindau disease. Medicine (Baltimore) **76:**381–391.
33. **Maxwell, P. H., M. S. Wiesener, G. W. Chang, S. C. Clifford, E. C. Vaux, M. E. Cockman, C. C. Wykoff, C. W. Pugh, E. R. Maher, and P. J. Ratcliffe.** 1999. The tumour suppressor protein VHL targets hypoxia-inducible factors for oxygen-dependent proteolysis. Nature **399:**271–275.
34. **Mukhopadhyay, D., B. Knebelmann, H. T. Cohen, S. Ananth, and V. P. Sukhatme.** 1997. The von Hippel-Lindau tumor suppressor gene product interacts with Sp1 to repress vascular endothelial growth factor promoter activity. Mol. Cell. Biol. **17:**5629–5639.
35. **Ohh, M., and W. G. Kaelin, Jr.** 1999. The von Hippel-Lindau tumor suppressor protein: new perspectives. Mol. Med. Today **5:**257–263.
36. **Ohh, M., C. W. Park, M. Ivan, M. A. Hoffman, T. Y. Kim, L. E. Huang, N. Pavletich, V. Chau, and W. G. Kaelin.** 2000. Ubiquitination of hypoxia-inducible factor requires direct binding to the beta-domain of the von Hippel-Lindau protein. Nat. Cell Biol. **2:**423–427.
37. **Ohh, M., R. L. Yauch, K. M. Lonergan, J. M. Whaley, A. O. Stemmer-Rachamimov, D. N. Louis, B. J. Gavin, N. Kley, W. G. Kaelin, Jr., and O. Iliopoulos.** 1998. The von Hippel-Lindau tumor suppressor protein is required for proper assembly of an extracellular fibronectin matrix. Mol. Cell **1:**959–968.
38. **Pal, S., K. P. Claffey, H. F. Dvorak, and D. Mukhopadhyay.** 1997. The von Hippel-Lindau gene product inhibits vascular permeability factor/vascular endothelial growth factor expression in renal cell carcinoma by blocking protein kinase C pathways. J. Biol. Chem. **272:**27509–27512.
39. **Pompe, T., F. Kobe, K. Salchert, B. Jorgensen, J. Oswald, and C. Werner.** 2003. Fibronectin anchorage to polymer substrates controls the initial phase of endothelial cell adhesion. J. Biomed. Mater. Res. **67A:**647–657.
40. **Regnault, V., C. Rivat, and J. F. Stoltz.** 1988. Affinity purification of human plasma fibronectin on immobilized gelatin. J. Chromatogr. **432:**93–102.
41. **Robinson, E. E., R. A. Foty, and S. A. Corbett.** 2004. Fibronectin matrix assembly regulates α5β1-mediated cell cohesion. Mol. Biol. Cell **15:**973–981.
42. **Ryan, H. E., J. Lo, and R. S. Johnson.** 1998. HIF-1 alpha is required for solid tumor formation and embryonic vascularization. EMBO J. **17:**3005–3015.
43. **Siemeister, G., K. Weindel, K. Mohrs, B. Barleon, G. Martiny-Baron, and D. Marme.** 1996. Reversion of deregulated expression of vascular endothelial growth factor in human renal carcinoma cells by von Hippel-Lindau tumor suppressor protein. Cancer Res **56:**2299–2301.
44. **Sinor, A. D., S. M. Irvin, C. S. Cobbs, J. Chen, S. H. Graham, and D. A. Greenberg.** 1998. Hypoxic induction of vascular endothelial growth factor (VEGF) protein in astroglial cultures. Brain Res. **812:**289–291.
45. **Stebbins, C. E., W. G. Kaelin, Jr., and N. P. Pavletich.** 1999. Structure of the VHL-elonginC-elonginB complex: implications for VHL tumor suppressor function. Science **284:**455–461.
46. **Stickle, N. H., J. Chung, J. M. Klco, R. P. Hill, W. G. Kaelin, Jr., and M. Ohh.** 2004. pVHL modification by NEDD8 is required for fibronectin matrix assembly and suppression of tumor development. Mol. Cell. Biol. **24:**3251–3261.
47. **Tallquist, M. D., and P. Soriano.** 2000. Epiblast-restricted Cre expression in MORE mice: a tool to distinguish embryonic versus extra-embryonic gene function. Genesis **26:**113–115.
48. **Tang, N., L. Wang, J. Esko, F. J. Giordano, Y. Huang, H. P. Gerber, N. Ferrara, and R. S. Johnson.** 2004. Loss of HIF-1α in endothelial cells disrupts a hypoxia-driven VEGF autocrine loop necessary for tumorigenesis. Cancer Cell **6:**485–495.
49. **Tian, H., S. L. McKnight, and D. W. Russell.** 1997. Endothelial PAS domain protein 1 (EPAS1), a transcription factor selectively expressed in endothelial cells. Genes Dev. **11:**72–82.
50. **Wu, M. H., E. Ustinova, and H. J. Granger.** 2001. Integrin binding to fibronectin and vitronectin maintains the barrier function of isolated porcine coronary venules. J. Physiol. **532:**785–791.